(37) R. F. Peterson, Jr., Yale University, private communication.
(38) D. Husain and L. J. Kirsch, *Trans. Faraday Soc.*, **67**, 2886–95 (1971).
(39) Aromatic triplets often undergo triplet–singlet transitions efficiently, particularly in the presence of xenon, so spin conservation can be a weaker requirement here than in systems studied earlier.
(40) Heats of formation of 116.7 and 67.6 kcal/mol for C_2H and C_4H_5 radicals respectively come from M. Cowperthwaite and D. H. Bauer, *J. Chem. Phys.*, **36**, 1743–53 (1962). The vinylacetylene triplet state energy, 90 kcal/mol, is taken from a calculation by M. Barfield, *ibid.*, **47**, 3831–36 (1967).
(41) R. M. Lambrecht, N. Furukawa, and A. P. Wolf, *J. Phys. Chem.*, **74**, 4605–08 (1970).
(42) $\Delta H_f[C_2H_4(T)]$ = 121 kcal/mol from R. S. Mulliken, *J. Chem. Phys.*, **33**, 1596–97 (1960), and $\Delta H_f[C_2H_2(T)]$ is estimated as 104 kcal/mol from C. C. Silicoiks, *Proc. R. Soc. London, Ser. A*, **242**, 411 (1957).

High-Temperature Ion–Molecule Chemistry. A Kinetic Study of Gas-Phase Reactions of Magnesium Atoms with D_3^+, Methanium, Ammonium, and *tert*-$C_4H_9^+$ Ions

P. L. Po and Richard F. Porter*

Contribution from the Department of Chemistry, Cornell University, Ithaca, New York 14853. *Received November 29, 1976*

Abstract: An apparatus is described for experimental investigations of ion–molecule reactions of metal vapors. The technique is applied to a study of charge and proton transfer reactions of D_3^+, CH_5^+, CH_4D^+, CD_4H^+, CD_5^+, $NH_nD_{4-n}^+$, and *tert*-$C_4H_9^+$ with Mg atoms. D_3^+ reacts with Mg(g) exclusively by a charge-transfer process. Methanium ions react with Mg(g) by charge- and proton-transfer mechanisms. Ammonium ion and *tert*-$C_4H_9^+$ react with Mg(g) by proton transfer. A lower bound of 8.37 eV is set on the proton affinity of the Mg atom. The bimolecular rate constant for the reaction of D_3^+ with Mg(g) and the composite rate constant for the reaction of CH_4D^+ with Mg(g) have been obtained from ion intensity data and ion residence times estimated from rate constants for known reactions ($k = 1.6 \pm 0.4 \times 10^{-9}$ cm^3 molecule^{-1} s^{-1} and $1.4 \pm 0.4 \times 10^{-9}$ cm^3 molecule^{-1} s^{-1}, respectively). Some mechanistic implications are drawn from kinetic measurements on the reaction of CH_4D^+ with Mg(g).

Current experimental research in gas-phase ion–molecule chemistry is generally limited to studies of substances with adequate volatility for operation at ordinary temperatures. For studies of ion–molecule reaction of metal atoms, high-temperature conditions are necessary and the technology for this type of investigation has not been fully developed. In this paper we report results of a "high-temperature" investigation of ion–molecule reactions of Mg(g) with a series of charge and proton transfer reagents including D_3^+, CH_5^+, CH_4D^+, CD_4H^+, CD_5^+, $NH_nD_{4-n}^+$ ($n < 4$), and *tert*-$C_4H_9^+$. The relative simplicity of the chemistry in these systems offers opportunity for examination and study of the fundamental aspects of processes occurring in ion–molecule reactions.

Experimental Section

The mass spectrometer used in these studies was constructed from a quadrupole mass filter from an EAI Quad 150A residual gas analyzer. The ion detector was a 14-stage electron multiplier. The ion source, capable of operating at a temperature as high as 900 °C, is illustrated in Figure 1. The ion–molecule reaction chamber was constructed entirely of stainless steel (type 304). The central section consisted of a piece of thin walled stainless steel tubing, 0.75-in. × 0.75-in. o.d. The top and bottom sections of the source were welded with vacuum tight seams to the main body of the source. A gas inlet tube was constructed from a piece of stainless steel tubing, 1.875-in. × 0.25-in. o.d. The electron entrance aperture and the ion exit aperture were 0.025-in. in diameter. The electron entrance aperture was located 1 cm below the ion exit aperture. The base of the source inlet stem was connected through a copper gasket to a stainless steel mounting plate. The source was electrically insulated from ground by a ceramic feed-thru. For most experiments the source was maintained at a potential of +22.5 V, and the drawout potential was held at −90 V. The filament used for the electron beam source was constructed from a piece of 0.001-in. × 0.025-in. rhenium ribbon. The electron accelerating voltage was set at −140 V with respect to the source. A repeller electrode was not employed in these experiments.

The source was heated radiatively from a spiral-shaped heating filament formed by stranding three 0.030-in. annealed tantalum wires. This filament was heated electrically by a set of transformers capable of delivering 190 A at 15 V. It was found that an output of 4 V and 35 A was sufficient to heat the source to 350 °C with constant temperature regulation. With the heating filament off, the ambient temperature reached 80 °C by radiation from the electron beam filament. A water-cooled grounded plate was located between the source and the mass filter assembly. This served as a heat shield to prevent heating of the quadrupole rods and as a collector of magnesium which had effused from the source. The temperature of the reactor was measured with a chromel–alumel thermocouple spot-welded to the base of the source. The thermocouple readings were calibrated against the melting points of indium and tin. The uncertainty in temperature was found to be ±3 °C.

Since the measurement of source pressure is an important quantity in these experiments, a series of flow calibration experiments were performed to correlate the source pressure with the pressure at the gas inlet line. A known quantity of gas was leaked into the source through a Nupro B-4MG metering valve for a known period of time. The pressure at the inlet was monitored with a McLeod gauge. Assuming the gas flow from the source is effusive, the gas pressure inside the source was calculated from the flow rate, the source temperature, and the standard effusion equation. For H_2 and D_2, a linear relationship was found between the inlet and source pressure to about 200 μm. For source pressures above 200 μm, some departure from linearity in the calibration curves was noted. However, most of the quantitative data reported in this paper were obtained from measurements at source pressures between 50 and 200 μm.

Magnesium was placed in the source as thin strips of metal in a configuration that did not block the ion exit and the electron entrance beams. In the absence of a reagent gas, Mg^+ was observed as the major ion in the spectrum. An ion signal of Mg_2^+, approximately 1% of the Mg^+ intensity, was also observed. As we note in Figure 2, the intensity of Mg^+ paralleled the temperature dependence of magnesium vapor (from JANAF tables[1]). The pressure of magnesium within the source was independently calibrated by measuring the rate of effusion of magnesium at 416 °C over a period of several hours. It was found that the vapor pressure of Mg at this temperature was about 10% higher than that calculated from the data in JANAF tables.[1] For a second method of calibration, a low pressure of Ne gas was introduced into the source and the relative intensities of Mg^+ and Ne^+ were recorded

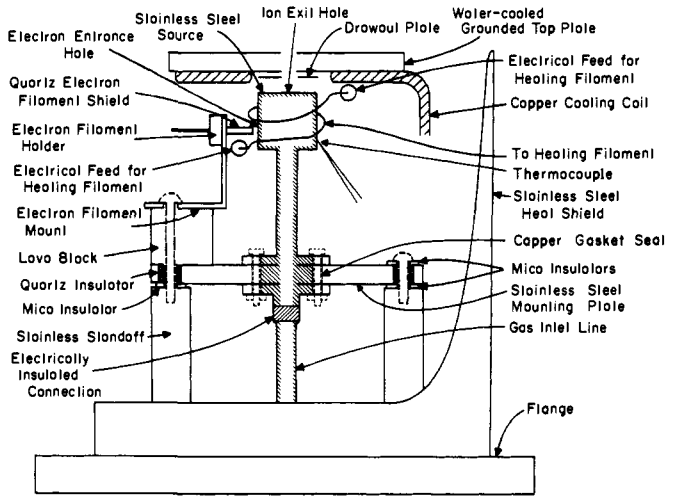

Figure 1. Experimental apparatus for investigation of ion-molecule reactions of metal atoms.

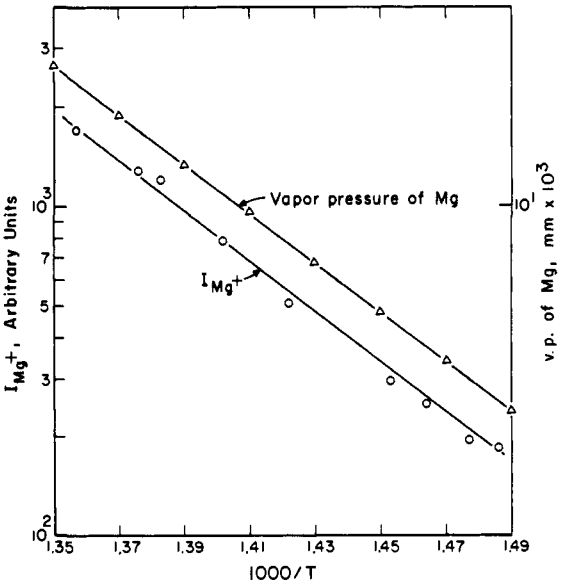

Figure 2. Experimental relationship between observed intensity of Mg^+ and calculated vapor pressure of Mg as a function of source temperature.

under conditions where charge transfer from Ne^+ to magnesium was not rapid. Using published electron impact cross sections at 140 V for neon[2] and magnesium[3] (0.78 and 3.7 Å^2, respectively), the pressure of magnesium was calculated to be about 20% higher than tabulated vapor pressure values. It should be noted that with the exponential dependence of vapor pressure of magnesium on temperature, it is possible through temperature variations of about 100 °C to change the density of magnesium atoms by a factor of around 30.

Since an ion repeller was not employed in these experiments, the residence times of ions were estimated from observations of a series of known ion-molecule reactions over a selected range of experimental conditions. In Figure 3 are shown intensity-pressure profile data from experiments with D_2 and D_2/CH_4 mixture at a source temperature of 350 °C. It is evident that the rate of reaction of D_2^+ with D_2 and the rate of deuteron transfer from D_3^+ to CH_4 were fast even at source pressures as low as 50 μm. Rate constants for the reactions

$$D_2^+ + D_2 \xrightarrow{k_1} D_3^+ + D \qquad (1)$$

$$D_3^+ + CH_4 \xrightarrow{k_2} CH_4D^+ + D_2 \qquad (2)$$

and

$$CH_5^+ + C_2H_4 \xrightarrow{k_3} C_2H_5^+ + CH_4 \qquad (3)$$

have been reported. Pierce and Porter[4] found that rate constant k_2 at 80 K (2.4×10^{-9} cm^3 molecule^{-1} s^{-1}) was not substantially different from that obtained by others at temperatures around 300 K. Thus we have assumed the rate constant k_2 is independent of temperature and estimated the residence time of D_3^+ for a range of conditions (see Figure 4). Although we know of no temperature dependence data for process 3, the rate constant reported by Fiaux et al.[5] ($k_3 = 1.5 \times 10^{-9}$ cm^3 molecule^{-1} s^{-1}) is typical of a fast ion-molecule reaction with zero activation energy. Thus we have assumed that reaction 3 is also independent of temperature. In our experiments we have chosen to use $C_2H_2D_2$ to simplify the interpretation of the processes occurring in the ion source. The residence times estimated for CH_4D^+ from the process

$$CH_4D^+ + C_2H_2D_2 \xrightarrow{k_4} C_2H_3D_2^+ + CH_3D \qquad (4)$$

are illustrated in Figure 4 at two temperatures. It is reasonable to suppose that the residence time of D_3^+ is shorter than that of CH_4D^+ because of the expected higher mobility of the lower mass species. The decrease in residence time for CH_4D^+ from measurements at 80 °C and measurements at 350 °C is also expected because of the increase in mobility of the ion at higher temperatures.

The relative mass discrimination factor for detection of D_3^+ (*m/e* 6) and CH_4D^+ (*m/e* 18) was obtained by the following procedure. Deuterium gas was introduced into the source at a pressure of about 100 μm. Under these conditions D_3^+ was the predominant ion species by reaction 1. From a separate metering valve, a small quantity of CH_4

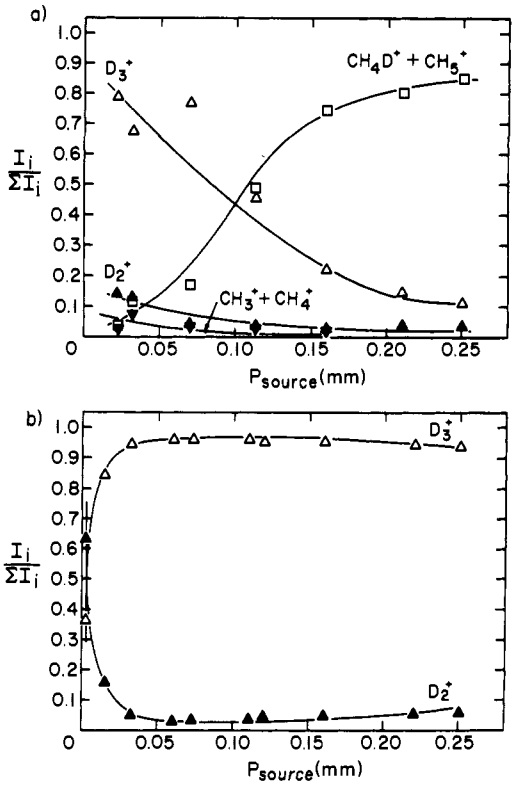

Figure 3. Ion intensity-pressure profile data for ions observed in (a) D_2-CH_4 mixture (100:1) at T = 350 °C and (b) pure D_2 at T = 350 °C.

(approximately 1 to 2 μm) was then injected into the source. The decrease in D_3^+ intensity due to reaction 2 was then compared to the compensated increase in the CH_4D^+ intensity. We have assumed that there is no substantial discrimination for ions in the mass range 15 to 32.

Before each experiment the empty source cell was degassed under vacuum at 900 °C. For these experiments it was essential that the interior surface of the reaction cell opposite the electron beam aperture be free of insulating surface films which are apparently not removed by the degassing process. To ensure proper operating conditions, it was useful to scratch the wall surface by inserting a small drill bit through the electron beam aperture. When the procedure was not

Table I. Rate Constants for the Reaction $D_3^+ + Mg \rightarrow Mg^+ + D_2 + D$

T, °C	P_{D_2}, μm	P_{Mg}, μm	P_{D_2}/P_{Mg}	$I_{Mg^+}/I_{D_3^+}$	κ	$\tau \times 10^5$, s	$k_7 \times 10^9$, cm^3 molecule^{-1} s^{-1}
340	90	0.21	4.3×10^2	0.11	48	2.3	1.4
	110	0.21	5.2×16^2	0.19	100	2.9	1.8
	130	0.21	6.2×10^2	0.22	140	3.4	1.8
	183	0.21	8.7×10^2	0.19	163	4.0	1.3
	233	0.21	1.1×10^3	0.20	219	4.4	1.2
324	233	0.10	2.3×10^3	0.087	203	4.4	1.2
347	43	0.29	1.5×10^2	0.052	7.7	0.90	1.3
355	41	0.41	1.0×10^2	0.11	11	0.85	2.0
374	37	0.94	3.9×10^1	0.16	6.4	0.75	1.4

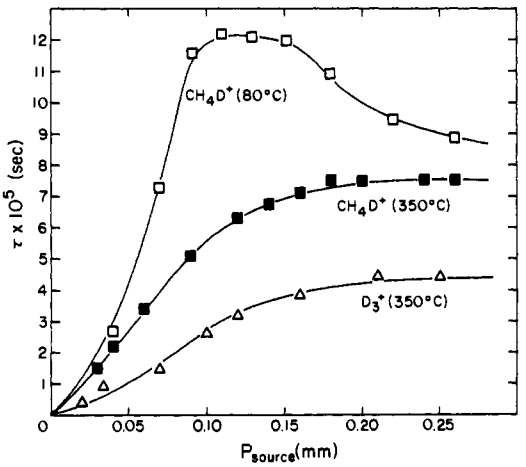

Figure 4. Estimated residence times in our source for D_3^+ in D_2–CH_4 mixture (200:1) at various pressures for T = 350 °C and for CH_4D^+ in D_2–CH_4–$C_2H_2D_2$ mixture (800:3:1) at 80 °C and at 350 °C.

followed, a substantial fraction of D_2 ions (from D_2) were apparently not formed in the central region of the source, and the rate of reaction 1 was diminished.

Magnesium ribbon was obtained from Mallinckrodt chemicals. Methane-d_4 (minimum purity of 99 atom % D) was obtained from Merck Sharp and Dohme. The research grade deuterium gas was obtained from Air Products Chemicals. The hydrogen was Fisher-brand high purity grade. All other gases were Matheson research grade.

Results

D_2–Mg System. We present first our observations of ion–molecule reactions occurring in gaseous mixtures of D_2 and Mg. Ion intensity data obtained from a series of measurements at different source temperatures and pressures are given in Table I. Under no experimental conditions was deuteron transfer to magnesium observed. At a constant temperature (340 °C) with Mg pressure invariant the Mg^+ intensity increased from 10 to 20% of the D_3^+ intensity as the deuterium pressure was increased from 90 to 233 μm. In these experiments the magnesium pressure ranged from 0.04 to 3% of the deuterium pressure while the intensity of Mg^+ was between 5 and 20% of the D_3^+ intensity. The formation of Mg^+ could be accounted for by charge transfer (or dissociative charge transfer) reactions of D_2^+ and/or D_3^+ with magnesium atoms, since both processes are thermodynamically possible. However, in the high deuterium pressure range, only one process appears dominant. It is convenient first to analyze the data assuming that the D_2^+ is the primary charge-transfer reagent by considering the following reaction sequence:

$$D_2^+ + D_2 \xrightarrow{k_1} D_3^+ + D \quad (1)$$

and

$$D_2^+ + Mg \xrightarrow{k_5} Mg^+ + D_2 \quad (5)$$

For this parallel reaction mechanism to be acceptable, the observed intensities of the product ions must be directly proportional to the partial pressures of their neutral precursors. Assuming the mechanism illustrated by eq 1 and 5, we can define

$$\kappa = (k_5/k_1) = (I_{Mg^+}/I_{D_3^+})(n_{D_2}/n_{Mg}) \quad (6)$$

If this mechanism is valid, the observed values of κ should satisfy two criteria. They should be sensibly constant under all experimental conditions and are expected to be of the order of unity. As we note in Table I, the observed κ changed markedly with source pressure of D_2. This indicates that in the high deuterium pressure range, reaction 5 is not the dominant charge-transfer mechanism.

Alternatively we must consider the consecutive reaction mechanism, i.e., reaction 1, followed by

$$D_3^+ + Mg \xrightarrow{k_7} Mg^+ + D_2 + D \quad (7)$$

As indicated in the "blank" study of deuterium at 350 °C, D_3^+ was over 90% of the total ionization at source pressures above 50 μm. Thus a kinetic analysis assuming reaction 7 would imply approximate constancy of the quantity $(I_{Mg^+})/(I_{D_3^+})$ in the high pressure range of these measurements. The data in Table I do, in fact, bear out this relationship. Thus we conclude that the ion–molecule mechanism consists of a fast reaction which depletes D_2^+ and a slower reaction which depletes D_3^+. Further analysis of the kinetics will be presented later.

D_2–CH_4–Mg System and CH_4–Mg System. The ion–molecule reactions occurring in gaseous mixtures of D_2 and CH_4 have been studied quite extensively (see references cited in ref 4). The major reactions involve the sequential process of reaction 1 followed by the deuteron transfer step

$$D_3^+ + CH_4 \xrightarrow{k_2} CH_4D^+ + D_2 \quad (2)$$

Under our experimental conditions, in the absence of magnesium vapor, the major species observed are D_3^+, CH_4D^+, a small intensity of CH_5^+ (typically around 15% of CH_4D^+), and very low intensities of CH_4^+, CH_3^+, and C_2 hydrocarbon ions. The CH_5^+ observed can be accounted for by two processes, namely

$$CH_4^+ + CH_4 \rightarrow CH_5^+ + CH_3 \quad (8)$$

$$CH_4D^+ + CH_4 \rightarrow CH_5^+ + CH_3D \quad (9)$$

When a D_2/CH_4 gas mixture was passed to a cell containing magnesium vapor, Mg^+, MgH^+, and MgD^+ were observed. In Figure 5 intensity–pressure profile data for this system (D_2/CH_4 = 90/1) for a temperature of 350 °C are shown.

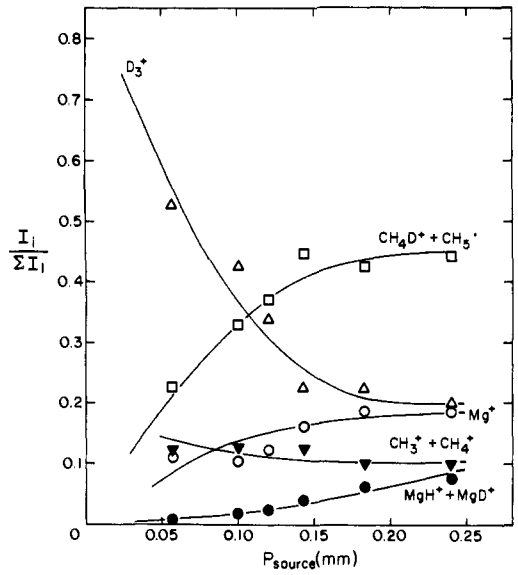

Figure 5. Ion intensity-pressure profile data for ions observed in D_2-CH_4-Mg mixture at T = 350 °C (D_2:CH_4 = 90:1, vapor pressure of Mg = 0.33 μm).

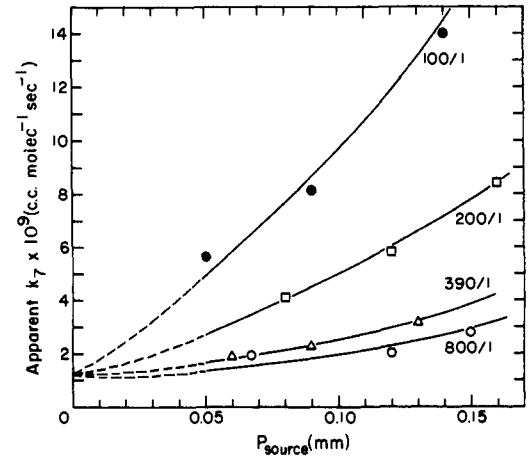

Figure 6. Calculations of apparent rate constant k_7 as a function of source pressure for a series of D_2/CH_4 reagent gases of different compositions at T = 348 °C (vapor pressure of Mg = 0.31 μm).

Since MgD^+ is not formed by deuteron transfer from D_3^+, it is concluded that the MgD^+ is formed predominantly through the reaction

$$CH_4D^+ + Mg \xrightarrow{k_{10}(D)} MgD^+ + CH_4 \quad (10a)$$

$$CH_4D^+ + Mg \xrightarrow{k_{10}(H)} MgH^+ + CH_3D \quad (10b)$$

Of course reaction 10b, proton transfer from CH_4D^+, also occurs. The intensities of CH_3^+ and CH_4^+ were small and remained relatively constant as a function of pressure in these experiments.

In these reactions D_3^+ is depleted by reactions with CH_4 and with Mg through reactions 2 and 7. If reaction 7 were the predominant reaction, leading to Mg^+, reactions 2 and 7 could be treated as a parallel reaction scheme. If this analysis were correct, then the ratio of product ion intensities would be

$$(I_{CH_4D^+})/(I_{Mg^+}) = (k_2/k_7)(n_{CH_4}/n_{Mg}) \quad (11)$$

Using eq 11 we have calculated apparent values of k_7 (using a known value of k_2) for a series of measurements with reagent gas mixtures with various D_2/CH_4 ratios. When k_7 was plotted against the source pressure (Figure 6), a substantial curvature was observed. This indicates that the intensity of Mg^+ remains high relative to CH_4D^+. We conclude therefore that in reagent gas mixtures with a high proportion of CH_4, Mg^+ is formed by the consecutive process involving reaction 2 followed by

$$CH_4D^+ + Mg \xrightarrow{k_{12}} Mg^+ + \text{products} \quad (12)$$

When the proportion of CH_4 is small, reaction 12 is apparently less important, and k_7 is sensibly constant over a range of source pressures.

Further analysis of reactions 10 and 12 was obtained from experiments using mixtures of H_2/CD_4 for the reagent gas. In Figure 7 is shown an ion intensity-temperature profile obtained in a series of measurements with a reagent gas of composition H_2/CD_4 = 200 for a fixed source pressure of 250 μm. As expected, when the concentration of magnesium was low, the dominant reaction was the formation of CD_4H^+ by proton transfer from H_3^+ to CD_4. The CD_5^+/CD_4H^+ ratio was

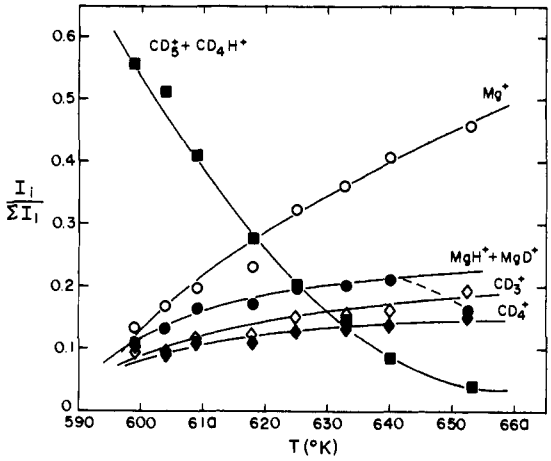

Figure 7. Ion intensity-temperature profile data for ions observed in H_2-CD_4-Mg mixture at a fixed source pressure of 250 μm (H_2:CD_4 = 200:1).

generally of the order of 0.1. In experiments with magnesium vapor present CD_4H^+ and CD_5^+ were depleted in reactions to yield Mg^+, MgH^+, and MgD^+. At temperatures near 640 K the sum of MgH^+ and MgD^+ intensities reached a maximum of 20% of the total ionization. At very high temperatures when the magnesium of CD_4 pressures were comparable, the Mg^+ is formed by competing charge-transfer reactions involving CD_4H^+ and H_3^+. The CD_3^+ and CD_4^+ intensities did not change perceptibly with temperature, indicating these ions were not participating signficantly in deuteron transfer reactions with Mg atoms.

From data obtained in these studies, it was possible to compare relative rates of D^+ and H^+ transfer to Mg from the partially deuterated methanium ions. Since H_3^+ (D_3^+) does not react with Mg by proton (deuteron) transfer the calculations of these isotope effects are greatly simplified. The pertinent data for the calculations are summarized in Table II. We have defined the relative probability that a $CH_nD_{5-n}^+$ ion will transfer a proton or a deuteron, p_H and p_D, respectively. For measurements in the $D_2/CH_4/Mg$ system, the quantity p_H is defined by the equation:

$$I_H(CH_nD_{5-n}^+)/I_D(CH_nD_{5-n}^+) \times (p_H)/(1-p_H) = (I_{MgH^+})/(I_{MgD^+}) \quad (13)$$

Table II. Isotope Distribution in Hydron Transfer Reactions of Ammonium and Methanium Ions with Mg

Mixture	Composition	T, °C	P_g, μm	$\frac{\Sigma I_H(NH_nD_{4-n}^+)}{\Sigma I_D(NH_nD_{4-n}^+)}$	$\frac{\Sigma I_H(CH_nD_{5-n}^+)}{\Sigma I_D(CH_nD_{5-n}^+)}$	I_{MgH^+}/I_{MgD^+}	$\frac{\Sigma I_D(CH_nD_{5-n}^+)}{\Sigma I_H(CH_nD_{5-n}^+)}$	I_{MgD^+}/I_{MgH^+}	p_H
D_2/NH_3	100/1	447	150	2.4 ± 0.5		2 6 ± 0.5			0.52
		457	93	4.4 ± 0.5		4.3 ± 1.1			0.50
D_2/CH_4	50/1	340	153		7.1 ± 0.1	7.8 ± 0.6			0.52
		412	270		6.9 ± 0.1	8.5 ± 0.8			0.55
	90/1	348	100		4.9 ± 0.1	5.0 ± 0.9			0.51
		348	240		6.0 ± 0.2	6.4 ± 0.9			0.52
	200/1	340	140		4.9 ± 0.1	5.4 ± 0.3			0.53
		363	130		4.9 ± 0.1	6.7 ± 0.4			0.58
H_2/CD_4	50/1	350	100				5.8 ± 0.1	2.7 ± 0.1	0.68
		374	167				6.2 ± 0.1	2.6 ± 0.1	0.71
	100/1	345	110				4.7 ± 0.1	2.5 ± 0.5	0.65
		370	140				4.7 ± 0.2	2.1 ± 0.3	0.69
	200/1	352	260				5.0 ± 0.1	2.3 ± 0.1	0.68
		367	260				4.5 ± 0.1	2.2 ± 0.1	0.68

Table III. Ion-Molecule Product Mass Spectra of Methane–Mg Mixtures at T = 350 °C

P_g, μm	P_{Mg}, μm	$I_{CH_3^+}/\Sigma I_i$	$I_{CH_4^+}/\Sigma I_i$	$I_{CH_5^+}/\Sigma I_i$	$I_{C_2H_3^+}/\Sigma I_i$	$I_{C_2H_5^+}/\Sigma I_i$	$I_{Mg^+}/\Sigma I_i$	$I_{MgH^+}/\Sigma I_i$	Mixture
6	0.33	0.26	0.21	0.28	0.05	0.20			Blank
7		0.29	0.30	0.17	0.04	0.08	0.10	0.02	With Mg
10		0.11	0.07	0.41	0.07	0.35			Blank
10		0.20	0.20	0.23	0.05	0.17	0.12	0.03	With Mg
18		0.05	0.03	0.46	0.07	0.39			Blank
22		0.10	0.10	0.34	0.05	0.22	0.13	0.06	With Mg
30		0.03	0.02	0.48	0.07	0.39			Blank
30		0.08	0.09	0.29	0.04	0.21	0.18	0.11	With Mg

where

$$I_H(CH_nD_{5-n}^+)/I_D(CH_nD_{5-n}^+) = (4I_{CH_4D^+} + 5I_{CH_5^+})/(I_{CH_4D^+})$$

Thus if the probability of protonation and deuteration were equal, p_H would be 0.50. By inverting the roles of hydrogen and deuterium atoms, similar mathematical equations can be used in the calculations of data from the $H_2/CD_4/Mg$ system. The list of the p_H values from all measurements is shown in Table II. It can be seen from these calculations that there is a substantial isotope effect, especially for the CD_4H^+ ion. It should be noted that the calculated p_H values were essentially independent of sample composition even though the proportions of CH_5^+ and CD_5^+ varied in these calculations somewhat. It is clear from these results that randomization of hydrogen and deuterium atoms does occur in the deuterated and protonated methane species.

In a separate set of experiments pure methane was used as a reagent gas. In the absence of magnesium vapor, the "blank" run indicated that the intensities of CH_5^+ and $C_2H_5^+$ were about 85% of total ionization at a source pressure of 18 μm, and the intensities of CH_3^+, CH_4^+, and $C_2H_3^+$ made up the additional 15%. With magnesium present in the source at its normal vapor pressure, Mg^+ and MgH^+ were also observed. The intensities of these ions increased with methane pressure, and the intensities of CH_5^+ and $C_2H_5^+$ were reduced relatively, indicating that these hydrocarbon species were reacting with Mg(g) (see Table III). Charge-transer reactions between Mg and hydrocarbon ions are apparently occurring in this system, but it is impossible to unravel the large number of competing processes.

D_2–NH_3–Mg System. We now discuss results of observations using D_2/NH_3 mixtures as reagent gas. The pertinent results of this investigation are given in Table IV. In this system ammonium ions are formed rapidly in the process

$$D_3^+ + NH_3 \rightarrow NH_3D^+ + D_2 \quad (14)$$

The scrambling reaction

$$NH_3D^+ + NH_3 \rightarrow NH_4^+ + NH_2D \quad (15)$$

also occurs rapidly. At source temperatures near 350 °C, in the absence/presence of Mg, extensive deuterium–hydrogen scrambling was observed yielding a complex ammonium ion spectrum consisting of NH_4^+, NH_3D^+, $NH_2D_2^+$, and a small intensity of NHD_3^+. Since deuteron transfer does not occur from D_3^+ to magnesium, the ammonium ions were the only ions of sufficient intensity to account for the proton (deuteron) transfer reaction leading to MgH^+ (MgD^+). Due to an apparent surface reaction between NH_3 or N_2 with Mg,[6] the volatility of Mg was reduced and the intensity of Mg^+ was substantially lower than in any of the experiments described above. This effect coupled with the thermal instability of NH_3 limited the range of pressure and temperature variation for these measurements. The results given in Table IV were obtained at a relatively high temperature necessary to enhance the volatility of magnesium. However it was possible to treat the isotope effects in the $H^+(D^+)$ transfer reactions

$$NH_nD_{4-n}^+ + Mg \xrightarrow{k_{16}(H)} MgH^+ + \text{product} \quad (16a)$$

$$NH_nD_{4-n}^+ + Mg \xrightarrow{k_{16}(D)} MgD^+ + \text{product} \quad (16b)$$

by the same procedure as used for analysis of the $CH_nD_{5-n}^+$ transfer process. These results and calculations are shown in Table II. From these data it appears that the probabilities of proton or deuteron transfer from $NH_nD_{4-n}^+$ to Mg are essentially equal.

When a mixture of Xe and NH_3 was used as a reagent gas, NH_4^+ is the dominant species through the consecutive processes

Table IV. Apparent Rate Constants for the Reaction $NH_nD_{4-n}^+ + Mg \rightarrow$ Products

Mixture	Composition	T, °C	P_g, μm	$(I_{MgH^+} + I_{MgD^+})/\Sigma I_{NH_nD_{4-n}^+}$	$I_{Mg^+}/I_{D_3^+}$	$n_{Mg\ calcd}$, molecule cm^{-3}	n_{Mg}, molecule cm^{-3}	k_{16}, cm^3 molecule^{-1} s^{-1}	$I_{MgH^+}/I_{NH_4^+}$	k_{16}, cm^3 molecule^{-1} s^{-1}
D_2/NH_3	100/1	447	150	7.4×10^{-3}	9.3×10^{-2}	1.7×10^{12}		6.5×10^{-11}		
				4.6×10^{-3}	5.1×10^{-2}	7.9×10^{11}		7.4×10^{-11}		
				3.1×10^{-3}	3.5×10^{-2}	6.2×10^{11}		7.3×10^{-11}		
				2.0×10^{-3}	2.1×10^{-2}	3.7×10^{11}		7.9×10^{-11}		
				1.6×10^{-3}	1.6×10^{-2}	2.9×10^{11}		8.0×10^{-11}		
		457	93	6.6×10^{-4}	4.6×10^{-3}	1.3×10^{11}		1.0×10^{-10}		
				9.2×10^{-4}	7.0×10^{-3}	2.0×10^{11}		9.2×10^{-11}		
				1.1×10^{-3}	9.1×10^{-3}	2.6×10^{11}		8.3×10^{-11}		
				1.3×10^{-3}	1.2×10^{-2}	3.3×10^{11}		7.4×10^{-11}		
				1.6×10^{-3}	1.4×10^{-2}	3.9×10^{11}		8.3×10^{-11}		
Xe/NH_3	20/1	400	90				3.7×10^{13}		4.8×10^{-4}	2.5×10^{-13}
	60/1	412	67				5.6×10^{13}		2.9×10^{-4}	1.4×10^{-13}
	60/1	353	100				5.9×10^{12}		6.0×10^{-4}	1.9×10^{-12}

Table V. Ion-Molecule Product Mass Spectra of Xe–i-C_4H_{10}–Mg[a] Mixtures[b]

T, °C	P_g, μm	$n_{i\text{-}C_4H_{10}}$, molecule cm^{-3}	n_{Mg}, molecule cm^{-3}	$n_{i\text{-}C_4H_{10}}/n_{Mg}$	$I_{C_3H_5^+}/\Sigma I_i$	$I_{C_3H_7^+}/\Sigma I_i$	$I_{C_4H_9^+}/\Sigma I_i$	$I_{Mg^+}/\Sigma I_i$	$I_{MgH^+}/\Sigma I_i$	Mixture
350	15				0.16	0.72	0.02			Blank
	11	3.4×10^{12}	5.1×10^{12}	0.67	0.13	0.56	0.00	0.20	0.06	With Mg
	47				0.15	0.61	0.14			Blank
	50	1.6×10^{13}	5.1×10^{12}	3.03	0.09	0.40	0.05	0.18	0.28	With Mg
	110				0.03	0.58	0.39			Blank
	110	3.4×10^{13}	5.1×10^{12}	6.66	0.03	0.23	0.13	0.19	0.41	With Mg
	130				0.04	0.53	0.43			Blank
	130	4.0×10^{13}	5.1×10^{12}	7.87	0.04	0.20	0.16	0.20	0.39	With Mg
350	93				0.05	0.63	0.32			Blank
400	97	2.8×10^{13}	3.7×10^{13}	0.75	0.03	0.10	0.02	0.43	0.42	With Mg

[a] Sample composition Xe:i-C_4H_{10} = 50:1. [b] Intensities of C_2 hydrocarbon ions not shown.

$$Xe^+ + NH_3 \rightarrow NH_3^+ + Xe \quad (17)$$

$$NH_3^+ + NH_3 \rightarrow NH_4^+ + NH_2 \quad (18)$$

Proton transfer to magnesium was also observed in this system. Due to the instability of ammonia and reduction of the Mg volatility under these conditions,[6] we were only able to obtain a few ion intensity measurements. These are given in Table IV.

Xe–i-C_4H_{10}–Mg System. In Table V are shown ion intensity–pressure profile obtained from a series of measurements using a mixture of Xe and i-C_4H_{10} as reagent gas. In the blank spectrum, the major ion species were $C_3H_7^+$ and $tert$-$C_4H_9^+$ and a small intensity of $C_3H_5^+$ at source pressure above 50 μm (at 350 °C). When magnesium vapor was present at 350 °C, MgH^+ increased to become the dominant ion species in the spectrum at pressures above 110 μm, while the Mg^+ intensity remained sensibly constant with increasing pressure. In the absence of Mg the major processes occurring at low pressures are presumably the exothermic charge transfer reaction

$$Xe^+ + i\text{-}C_4H_{10} \rightarrow C_3H_7^+ + Xe + CH_3 \quad (19)$$

followed by the hydride abstraction reaction

$$C_3H_7^+ + i\text{-}C_4H_{10} \rightarrow tert\text{-}C_4H_9^+ + C_3H_8 \quad (20)$$

Proton transfer to Mg could occur through the reaction

$$C_3H_7^+ + Mg \rightarrow MgH^+ + C_3H_6 \quad (21)$$

or

$$tert\text{-}C_4H_9^+ + Mg \rightarrow MgH^+ + C_4H_8 \quad (22)$$

or both. The observed data cannot be explained solely by the two competitive steps, reactions 20 and 21, since the MgH^+ intensity reaches over 40% of the total ion intensity of hydrogen-bearing species when the pressure of C_4H_{10} exceeds that of Mg by a factor of 10 at the highest source pressure. The simplest interpretation of these results is that at high source pressures $tert$-$C_4H_9^+$ forms rapidly by reaction 20 and is then diminished by reaction 22.

Kinetic Analyses. All bimolecular rate constants reported here are indexed according to their reaction equation numbers. Rate data for reaction 7 were treated assuming pseudo-first-order kinetics for the disappearance of D_3^+. With this assumption the integrated rate expression for the disappearance of D_3^+ is given by

$$-RT \ln\{(I_{D_3^+})/(I_{D_3^+} + I_{Mg^+})\} = k_7 P_{Mg} \tau_{D_3^+} \quad (23)$$

where $\tau_{D_3^+}$ is the residence time for D_3^+ ion, P_{Mg} is the vapor pressure of Mg in the source at temperature T, and R is the gas constant. Values k_7 calculated from a series of experimental conditions are shown in Table I. It is noted that these values are insensitive to source temperature and pressure and yield an average value of $k_7 = 1.6 \pm 0.4 \times 10^{-9}$ cm^3 molecule^{-1} s^{-1}. The data indicated in Figure 5 can also be used to obtain k_7 directly through eq 11, provided the calculations are based on measurements obtained when the source pressure of CH_4 was comparable to that of Mg. A rough extrapolation of the data obtained with the reagent gas of composition D_2/CH_4 = 800/1 yields a rate constant of 1.2×10^{-9} cm^3 molecule^{-1} s^{-1}.

Rate data for the D_2/CH_4/Mg system were treated similarly using an integrated pseudo-first-order rate expression for the disappearance of CH_4D^+. The integral reaction rate constant, k_t, is given in the expression

$$-RT \ln\{(I_{CH_4D^+} + I_{CH_5^+})/(I^0)\} = k_t P_{Mg} \tau_{CH_4D^+} \quad (24)$$

Table VI. Rate Constants for the Reactions $CH_4D^+ + Mg \rightarrow$ Products at $T = 350$ °C

D_2/CH_4 composition	P_g, μm	$I_{CH_5^+}/I_{CH_4D^+}$	$\{I_{Mg^+}/(I_{MgH^+} + I_{MgD^+})\}_{obsd}$	$I_{MgH^+}/I_{CH_4D^+}$	$I_{MgD^+}/I_{CH_4D^+}$	$\tau \times 10^5$, s
20/1	110	0.96	2.0			
	210	1.75	1.9			
90/1	183	0.26	3.0	0.16	0.028	7.5
	280	0.55	2.2	0.23	0.034	7.5
101/1	50	0.22	22.0	0.057	0.014	2.8
	90	0.16	9.2	0.12	0.027	5.0
	140	0.20	4.7	0.31	0.058	6.7
200/1	80	0.12	13.0	0.10	0.022	4.6
	100	0.12	10.0	0.10	0.023	5.4
	160	0.13	5.3	0.28	0.066	7.1
	200	0.15	3.5	0.27	0.064	7.5

	k_t, cm^3 molecule^{-1} s^{-1}	k_{12}, cm^3 molecule^{-1} s^{-1}	k_{10}(H), cm^3 molecule^{-1} s^{-1}	k_{10}(D), cm^3 molecule^{-1} s^{-1}
90/1	1.0×10^{-9}	6.5×10^{-10}	2.8×10^{-10}	6.9×10^{-11}
	1.1×10^{-9}	7.2×10^{-10}	3.1×10^{-10}	7.7×10^{-11}
101/1	1.2×10^{-9}	7.8×10^{-10}	3.3×10^{-10}	8.3×10^{-11}
	1.2×10^{-9}	7.8×10^{-10}	3.3×10^{-10}	8.3×10^{-11}
	1.8×10^{-9}	1.2×10^{-9}	5.0×10^{-10}	1.3×10^{-10}
200/1	1.3×10^{-9}	8.3×10^{-10}	3.5×10^{-10}	8.8×10^{-11}
	1.1×10^{-9}	7.2×10^{-10}	3.1×10^{-10}	7.6×10^{-11}
	1.8×10^{-9}	1.2×10^{-9}	5.0×10^{-10}	1.3×10^{-10}
	1.7×10^{-9}	1.1×10^{-9}	4.9×10^{-10}	1.2×10^{-10}

where

$$I^0 = I_{CH_4D^+} + I_{CH_5^+} + I_{Mg^+} + I_{MgH^+} + I_{MgD^+}$$

and

$$k_t = k_{12} + k_{10}(H) + k_{10}(D) \quad (25)$$

To calculate I^0 it is necessary to know the branching ratios I_{Mg^+}:I_{MgH^+}:I_{MgD^+} resulting only from reactions 12, 10a, and 10b. These ratios were obtained from observations using a reagent gas with high CH_4/D_2 ratio (1/20). Under these conditions the extent of reaction 7 was small, accounting for about 10% of the Mg^+ intensity. The branching rate constants are related through the relationship

$$(I_{Mg^+})/(I_{MgH^+} + I_{MgD^+}) = k_{12}/(k_{10}(H) + k_{10}(D)) = 1.8 \pm 0.2 \quad (26)$$

Values of k_t calculated from eq 24 are indicated in Table VI. The results are reasonably concordant over a range of experimental conditions. Using eq 26 and the observed hydrogen–deuterium isotope effects (Table II), we obtain separate constants for each process. These results are given in Table VI. The average values are $k_t = 1.4 \pm 0.4 \times 10^{-9}$ cm^3 molecule^{-1} s^{-1}, $k_{12} = 8.9 \pm 2.2 \times 10^{-10}$ cm^3 molecule^{-1} s^{-1}, $k_{10}(H) = 3.8 \pm 0.9 \times 10^{-10}$ cm^3 molecule^{-1} s^{-1}, $k_{10}(D) = 9.5 \pm 2.4 \times 10^{-11}$ cm^3 molecule^{-1} s^{-1}.

Due to apparent reduction in magnesium vapor pressure in experiments with NH_3, the rate constants for reactions 16a and 16b could only be roughly estimated (see Table IV). The real number density of magnesium atoms was estimated from rate data for reaction 7 using the observed D_3^+ and Mg^+ intensities. Assuming the residence time for the ammonium ion is comparable to that for CH_4D^+, we obtain $k_{16}(H) \approx 8 \times 10^{-11}$ cm^{-3} molecule^{-1} s^{-1}. Calculations using the vapor pressure of Mg taken from the JANAF Tables[1] give a lower limit of 10^{-13} cm^3 molecule^{-1} s^{-1} for the rate constant.

Calculations indicate the polarizability of Mg atoms is in the range 7–11 Å^3.[7,8] The Langevin rate constant for reaction 7 and the composite rate constant for reactions 10a, 10b, and 12 are calculated to be 2.8×10^{-9} to 3.5×10^{-9} cm^3 molecule^{-1} s^{-1} and 1.9×10^{-9} to 2.4×10^{-9} cm^3 molecule^{-1} s^{-1}, respectively.

We assign the major fraction of our experimental uncertainty in rate constants to estimates of ion residence times. Residence times estimated for D_3^+ in D_2 in the low-pressure collisionless regime (less than 10 μm) indicate the ion kinetic energy is above thermal suggesting the presence of a small residual field in the ion source (between about 0.5 to 1.0 V/cm). This is probably due to a combination of effects from the electron beam filament and the drawout electrode even though in the high-pressure regime the reactant ions are probably nearly thermalized by collisions with the neutral molecules. Since the reactant ions may still have a slight excess initial energy, our rate constants measured do not correspond precisely to thermal values.

Discussion

Analyses of our results follow observations that (1) D_3^+ reacts with Mg atoms exclusively by charge transfer, (2) CH_4D^+ reacts with Mg atoms by charge and proton (deuteron) transfer, and (3) *tert*-$C_4H_9^+$ and NH_4^+ react with Mg atoms predominantly by proton transfer. We will discuss these observations in terms of the kinetic and thermodynamic aspects of these reactions.

Since the thermodynamic stabilities of the proton and charge-transfer reagents investigated are known,[9-12] we can establish an energy level diagram referenced to the Mg atom and the H^+ ion (Figure 8). It should be noted that the energy separation between $Mg(^1S_0) + H^+$ and each reaction energy is equivalent to the proton affinity of the conjugate base of the reactant ions. In Figure 8 we give tentative locations of the known states of MgH^+ [13,14] with respect to the $(Mg^+ + H)$ system.[15] Only three states of MgH^+ (the ground $^1\Sigma$ and excited $^1\Sigma$ and $^1\Pi$ states) have been reported.[13,14] The locations of the lowest triplet states are unknown to our knowledge. We will discuss later the estimation of the dissociation energies of the two $^1\Sigma$ states.

We note first that the reaction $D_3^+(H_3^+)$ with Mg atoms places the reaction products substantially above the dissociation limit of ground state MgH^+ but below the limit for the excited $^1\Sigma$ state. Thus we may conclude that deuteron (proton) transfer from $D_3^+(H_3^+)$ to Mg is not expected even though such a process is thermodynamically allowed. The occurrence

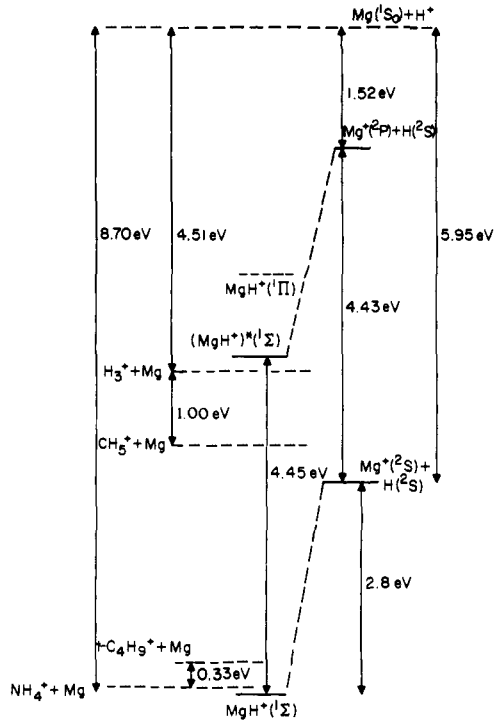

Figure 8. Energy level diagram connecting the states of MgH^+ with $Mg^+ + H$ and $Mg + H^+$ and the total energies of several charge and proton transfer reactions.

of deuteron (proton) transfer to Mg would necessarily imply a high degree of excitation in the neutral product of the reaction. It should be noted that Smith and Futrell[16] reported that D_3^+ is vibrationally deactivated in less than ten collisions with D_2. This condition should be applicable to our reaction conditions for source pressures above 100 μm.

We consider next possible mechanisms of the reaction of CH_5^+ with Mg atoms. The total energy of the reaction places the products above the ground state MgH^+ dissociation limit. We propose for the charge transfer reaction a near resonance electron transfer process

$$CH_5^+ + Mg \rightarrow [CH_5] + Mg^+ \qquad (27)$$

with the excess energy of the reaction dissipated in the neutral reaction products, $CH_4 + H$ or $CH_3 + H_2$. For either set of products, the reaction is exoergic to the extent of about 11 kcal/mol.[17] From the preceding analysis the occurrence of proton transfer in this system seems unique and some speculation is justified. Observation of a collisionally stabilized MgH^+ ion in our instrument would imply an ion lifetime following formation of the order of 0.1–1 μs. The product of the reaction would not have a sufficient lifetime to undergo collisions if it is formed near or above its dissociation limit. One possibility is that MgH^+ is stabilized by a chemiluminescent process from an excited state. However, since there does not appear to be a bound excited state of MgH^+ in the proper energy domain, this possibility seems unlikely. An alternate explanation which seems more probable is that the methane molecule formed in the reaction is in a state of vibrational excitation.[5] To examine this possibility, let us consider the kinetic implication of reactions 10a and 10b in reference to the structure of CH_5^+ which is known only from theoretical calculations. Results of CNDO calculations[18] indicate an ion structure of C_s symmetry (Figure 9) with three "normal" carbon hydrogen bonds and a three-center bond

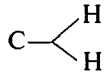

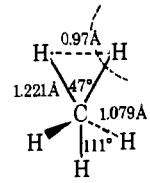

Figure 9.

Assuming this structure we can visualize a direct process in which a proton from the three-center bond is transferred to a magnesium atom leaving the product CH_4 molecule in a distorted configuration.[5] Further CNDO calculations[19] for this distorted methane structure using unchanged coordinates from the CH_5^+ structure[20] (Figure 9) indicate a distortion energy of about 20 kcal/mol with respect to the stable CH_4 configuration. An excitation energy of 20 kcal/mol or more in the CH_4 formed in reactions 10a and 10b would be compensated by lowering the energy of MgH^+ below the dissociation limit. It may be noted that for the thermoneutral proton transfer process

$$CH_4D^+ + CH_4 \rightarrow CH_5^+ + CH_3D \qquad (9)$$

a proton jump mechanism similar to the one described above could not take place for ground state species without violating energy conservation. Pierce and Porter[4] have explained the observed increase in reaction rate of (9) with decreasing temperature by proposing that the mechanism involves a "thermalized" complex intermediate whose lifetime increases with decreasing temperature. We cannot rule out the possibility that reaction 10 proceeds by a complex mechanism.

The total energies of the reactions of *tert*-$C_4H_9^+$ and NH_4^+ with Mg atoms place the reaction products below the MgH^+ ground state dissociation limit (see Figure 8). The *tert*-$C_4H_9^+$ formed by reaction 20 is expected to be close to its ground state energy since that reaction is only exoergic by about 1.5 kcal/mol.[21] Reaction 14 leading to the formation of NH_3D^+ is more exoergic ($\Delta H \sim -96$ kcal/mol[22]). However, at high source pressures in experiments with $D_2/NH_3/Mg$ (above 100 μm), $NH_nD_{4-n}^+$ undergoes a number of unreactive collisions with D_2 and proton (deuteron) transfer reactions with NH_3. Thus collisional deactivation of the ammonium ion prior to its reaction with Mg(g) is anticipated. From these measurements we place the proton affinity of magnesium above that for *i*-C_4H_8 (8.37 eV[11]) but probably slightly lower than that for NH_3 (8.70 eV[12]). (The rate constant for 16 suggests a slight endothermicity for the reaction.) This indicates the dissociation energy of MgH^+ (to $Mg^+ + H$) is above the estimated value of 2.1 eV given by Herzberg.[13] Our results appear to be more consistent with a $D_0^0(MgH^+) = 2.8$ eV obtained from a linear extrapolation of vibrational energy levels. From the observed ($^1\Sigma$–$^1\Sigma$) transition of MgH^+ [13,14] and the energy separation of the ^2P and ^2S states of Mg^+,[15] a dissociation energy of about 2.8 eV is obtained for the first excited singlet state of MgH^+.

Product distributions of the hydron-transfer reactions between CH_4D^+ and Mg(g) indicate that proton transfer (on a per atom basis) is slightly favored over deuteron transfer. In the reactions of CD_4H^+ with Mg(g) proton transfer is favored to a considerable extent over deuteron transfer. For $NH_nD_{4-n}^+$ the probability of hydron transfer is approximately the same for both isotopes. Similar experimental results for the methanium ions have been reported by Sefcik et al.[23] and later by Smith and Futrell.[24] Sefcik et al. proposed that the observed chemical equivalency of the hydrons in the presumed C_s structure of the methanium ion was due to internal rearrangement of the ion via a C_{2v} intermediate.[25] This barrier for rearrangement has been calculated to be about 6 kcal/

mol,[20] while reaction 2 forming CH_4D^+ is estimated to be exoergic by 23 kcal/mol.[26] Therefore it is highly likely that internal rearrangement would occur during the initial formation of the methanium ion. Neither our results nor those of previous workers[23,24] can definitely establish the structure of the methanium ion. However, we feel that our results show a discernible isotope effect for CD_4H^+ which may reflect the uniqueness of this structure.

Acknowledgment. We are grateful to Mr. Tom Savino for his assistance with the CNDO calculations. We are grateful for support of this work by the National Science Foundation (Grant GH-33637) through the Materials Science Center, Cornell University. P. L. Po wishes to thank the Proctor and Gamble Co. for its fellowship.

References and Notes

(1) D. R. Stull and H. Prophet et al., *Natl. Stand. Ref. Data Ser., Natl. Bur. Stand.*, **No. 37** (1971).
(2) D. Rapp and P. Englander-Golden, *J. Chem. Phys.*, **43**, 1464 (1965).
(3) Y. Okuno, K. Okuno, Y. Kaneko, and I. Kanomata, *J. Phys. Soc. Jpn.*, **29**, 164 (1970).
(4) R. C. Pierce and R. F. Porter, *J. Phys. Chem.*, **78**, 93 (1974).
(5) A. Fiaux, D. L. Smith, and J. H. Futrell, *Int. J. Mass Spectrom. Ion Phys.*, **15**, 9 (1974).
(6) P. Sthapitanonda and J. L. Margrave, *J. Phys. Chem.*, **60**, 1628 (1956).
(7) P. L. Altick, *J. Chem. Phys.*, **40**, 238 (1964).
(8) W. C. Stwalley, *J. Chem. Phys.*, **54**, 5417 (1971).
(9) P. F. Fennelly, R. S. Hamsworth, H. I. Schiff, and D. K. Bohme, *J. Chem. Phys.*, **59**, 6405 (1973).
(10) W. A. Chupka and J. Berkowitz, *J. Chem. Phys.*, **54**, 4256 (1971).
(11) W. Tsang, *J. Phys. Chem.*, **76**, 143 (1972); F. P. Lossing and G. P. Semeluk, *Can. J. Chem.*, **48**, 955 (1970).
(12) R. Yamdagni and P. Kebarle, *J. Am. Chem. Soc.*, **98**, 1320 (1976).
(13) G. Herzberg, "Molecular Spectra and Molecular Structure, I. Spectra of Diatomic Molecules", 2nd ed, Van Nostrand, Princeton, N.J., 1955.
(14) W. J. Balfour, *Can. J. Phys.*, **50**, 1082 (1972).
(15) C. E. Moore, *Natl. Stand. Ref. Data Ser., Natl. Bur. Stand.*, **No. 35** (1971).
(16) D. L. Smith and J. H. Futrell, *Chem. Phys. Lett.*, **40**, 229 (1976).
(17) Calculations based on proton affinity of CH_5^+ obtained from ref 7 and heats of formation from J. L. Franklin, J. G. Dillard, H. M. Rosenstock, J. T. Herron, K. Draxl, and F. H. Field, *Natl. Stand. Ref. Data Ser., Natl. Bur. Stand.*, **No. 26** (1969).
(18) A. Gambo, G. Morosi, and M. Simonetta, *Chem. Phys. Lett.*, **3**, 20 (1969).
(19) Calculations using standard CNDO/2 computer program, see J. A. Pople and D. L. Beveridge. "Approximate Molecular Orbital Theory", McGraw-Hill, New York, N.Y., 1970.
(20) O. V. Dyczmons, V. Staemmler, and W. Kutzelnigg, *Chem. Phys. Lett.*, **5**, 361 (1970).
(21) Calculations based on heat of formation data, see ref 17.
(22) Calculations based on proton affinities of H_2 and NH_3, see ref 9 and 12.
(23) M. D. Sefcik, J. M. S. Henis, and P. P. Gasper, *J. Chem. Phys.*, **61**, 4321 (1974).
(24) R. D. Smith and J. H. Futrell, *Chem. Phys. Lett.*, **36**, 545 (1975).
(25) S. Ehrenson, *Chem. Phys. Lett.*, **3**, 585 (1969).
(26) Calculations based on proton affinities of H_2 and CH_4, see ref 9 and 10.

Thermodynamics of Electrolytes. 7. Sulfuric Acid

Kenneth S. Pitzer,* Rabindra N. Roy, and Leonard F. Silvester

Contribution from the Department of Chemistry and the Lawrence Berkeley Laboratory, University of California, Berkeley, California 94720. *Received March 9, 1977*

Abstract: Although the thermodynamic properties of sulfuric acid above 0.1 M and near 25 °C are well established numerically, they have not been represented accurately by equations which are based upon the ionic species present, H^+, HSO_4^-, and SO_4^{2-}. We have developed and fitted such equations over the range from 0 to 6 M in a system compatible with those for fully dissociated, strong electrolytes. The enthalpy is treated as well as the activity and osmotic coefficients. These equations also establish the solute standard state and the relationship between the properties of sulfuric acid in that state with those for the pure acid. Among the results obtained (for 25 °C) are the dissociation constant 0.0105 and the heat of dissociation −5.61 kcal mol^{-1} for HSO_4^- and the entropy of SO_4^{2-}, 4.2 ± 0.2, and of HSO_4^-, 32.1 ± 0.3 cal K^{-1} mol^{-1}. Also for the reaction $H_2SO_4(l) = 2H^+(aq) + SO_4^{2-}(aq)$, $\Delta H^\circ = -22844$, $\Delta G^\circ = -12871$ cal mol^{-1}.

In view of the great practical importance of sulfuric acid, it is desirable to have the most accurate and convenient expression of its thermodynamic properties. Above 0.1 M these properties are now well established,[1-6] but there is still considerable uncertainty about the properties of very dilute solutions and the related solute standard state. In this research we have the dual purposes first to establish as accurately as possible the thermodynamic properties of dilute sulfuric acid and second to provide a convenient yet accurate analytical representation of the properties of this acid in a form compatible with that used for other electrolytes[7-9] and over as wide a range of concentration as is feasible.

The thermodynamic treatment of sulfuric acid has been unusually difficult because the dissociation constant of HSO_4^- lies in the most troublesome region where methods fail that were successful for weaker acids.[10,11] The preceding paper of this series[12] considered this general problem with phosphoric acid as an example. Sulfuric acid is even more troublesome in view of the higher charge on the sulfate ion and the correspondingly larger changes in its activity coefficient.

General Equations

The statistical mechanical basis for the form of equation for a complex electrolyte was given in the first paper of this series.[7] The general framework is that of the McMillan-Mayer theory of solutions and the equation relating intermolecular forces and distributions to the osmotic pressure.[13] Our basic equation is

$$\frac{G^{ex}}{RT} = n_w f(I) + \frac{1}{n_w}\sum_{ij}\lambda_{ij}(I)n_i n_j + \frac{1}{n_w^2}\sum_{ijk}\mu_{ijk}n_i n_j n_k \quad (1)$$

where G^{ex} is the excess Gibbs energy for a solution containing n_w kg of solvent and n_i, n_j, etc., moles of solute species i, j, etc. Here $f(I)$ is a function of ionic strength (and temperature and solvent properties) expressing the effect of long-range electrostatic forces between ions and including, of course, the Debye-Hückel limiting law. Short-range interactions of solute species lead to the terms $\lambda_{ij}(I)$ for binary interactions and μ_{ijk} for ternary interactions; the theoretical basis for expecting an ionic-strength dependence for λ_{ij} was given earlier[7] and this has been fully confirmed empirically. The λ and μ matrices are symmetric, i.e., $\lambda_{ij} = \lambda_{ji}$, etc.

Equations for Sulfuric Acid

The intermediate thermodynamic derivations of activity and osmotic coefficients and the definitions of experimentally